Exchange-bias-modulated inverse superconducting spin switch in $CoO/Co/YBa_2Cu_3O_{7-\delta}/La_{0.7}Ca_{0.3}MnO_3$ thin film hybrids

N. M. Nemes*
GFMC, Departamento de Fisica Aplicada III, Universidad Complutense de Madrid, 28040 Madrid, Spain and Instituto de Ciencia de Materiales de Madrid, Consejo Superior de Investigaciones Cientificas, 28049 Cantoblanco, Spain

C. Visani, Z. Sefrioui, C. Leon, and J. Santamaría
GFMC, Departamento de Fisica Aplicada III, Universidad Complutense de Madrid, 28040 Madrid, Spain

M. Iglesias, F. Mompean, and M. García-Hernández
Instituto de Ciencia de Materiales de Madrid, Consejo Superior de Investigaciones Cientificas, 28049 Cantoblanco, Spain
(Received 3 June 2009; revised manuscript received 18 August 2009; published 15 January 2010)

We examine the interplay between ferromagnetism and superconductivity in bilayer and trilayer heterostructures based on Co, $YBa_2Cu_3O_{7-\delta}$ (YBCO), and $La_{0.7}Ca_{0.3}MnO_3$ (LCMO) thin films grown on $SrTiO_3$ substrates with typical thicknesses of 10–15 nm. We have measured magnetoresistance below the resistive-superconducting onset of the YBCO. Naturally oxidized antiferromagnetic CoO top layer films give rise to pronounced exchange bias, modifying the coercive field of the Co by several hundred Oe. This allows separating effects at coercivity, such as stray fields, from those of parallel vs. antiparallel magnetic alignment between top and bottom ferromagnetic layers. In bilayers of Co/YBCO and of LCMO/YBCO, we observe a small magnetoresistance peak centered at the coercive field of the ferromagnetic layer of at most 20%, which we attribute to the effect of stray fields generated in the domain state of the ferromagnet. In the case of the $CoO/Co/YBCO/LCMO/SrTiO_3$ trilayer, aside from the peaks at coercivity, we observe a well-defined plateau of the magnetoresistance extending between the coercive fields of the LCMO and Co, with a width that is modified by the exchange-biased Co layer. Reactivity between Co and YBCO at the interface gives rise to a progressive deterioration in the superconducting transition temperature. Aged samples display magnetoresistance peaks at the coercive fields of the Co and LCMO characteristic of stray fields without the magnetoresistance *plateau* between them.

DOI: 10.1103/PhysRevB.81.024512 PACS number(s): 74.78.Fk, 74.72.−h, 75.70.Cn

I. INTRODUCTION

In recent years, there has been a surge of interest in the study of the interplay between ferromagnetism (F) and superconductivity (*S*) in thin film hybrids.[1,2] At the F/*S* interface, there is a strong interplay between both long-range orders which gives rise to a variety of interesting effects and phenomena. The so-called superconducting spin valve has received particular attention. This is a trilayer ferromagnet (F)-superconductor (*S*)-ferromagnet (F) structure where the superconductivity is modulated by the relative orientation of the magnetizations of the F layers which can be switched independently.

In proximity-coupled structures, superconductivity is promoted for antiparallel (AP) orientation as a result of the cancellation of the effect of the exchange field over the coherent volume.[3–8] Resistance decreases when the magnetic configuration is changed from parallel (P) to antiparallel (AP), at temperatures fixed along the resistive transition. On the other hand, a number of reports show a resistance increase when going to the AP alignment, suggesting that superconductivity might be favored in the P state.[9–11] The term "inverse" superconducting spin switch (SSS) has been coined to describe this behavior.[10] Its origin has been a subject of intense debate in recent years. Some reports point out the possibility of spin-dependent transport effects, particularly for strong ferromagnets.[9–11] A competing interpretation outlines the importance of stray fields, generated in the domain state of the ferromagnet, depressing superconductivity.[12,13]

Spin-dependent effects are expected to show up as a difference between transport properties of AP and P configurations. On the contrary, ferromagnetic domains at the interface influence superconductivity primarily at coercivity.[13–15] For Bloch-type domain walls, magnetization rotates out of plane between neighboring domains, generating perpendicular stray fields, which may strongly depress superconductivity. Positive magnetoresistance (MR) peaks are thus expected at coercivity in resistance vs. field, $R(H)$, sweeps. Quite frequently, the AP state is established in a narrow-field interval between the different coercivities of top and bottom ferromagnetic layers often due to different growth properties, thus it becomes a difficult task to distinguish between the two mechanisms.

A key step to separate spin-dependent transport from the effect of stray fields is to tailor well-defined AP states that extend over wide magnetic field intervals, preferably together with sharp magnetization switching. In structures combining transition-metal ferromagnets and low-T_c superconductors, this has been accomplished by means of pinning the magnetization of one of the layers via exchange bias in exchange spring structures.[12,16] In these cases, the antiferromagnet (AF) of the AF/F exchange bias structures was produced by *in situ* oxidation of one of the F layers. In this way, Steiner and Ziemann[12] and also Stamopoulos *et al.*[13] showed

MR peaks at the coercive fields due to the action of stray fields.

In heterostructures based on oxide (colossal magnetoresistance) ferromagnets and high-T_c superconductors (cuprates), the situation is more complicated. Such is the case of $La_{0.7}Ca_{0.3}MnO_3$ (LCMO)/$YBa_2Cu_3O_{7-\delta}$ (YBCO)/$La_{0.7}Ca_{0.3}MnO_3$ (LCMO) trilayers, where the inverse SSS was first reported.[9] The YBCO/LCMO interface displays interesting F/*S* interplay phenomena.[13,17–22] Natural oxidation cannot be used to produce an AF layer and incorporating an extra AF layer has so far shown to degrade the superconducting properties of the heterostructures.[23] Nevertheless, extrapolating the results obtained for transition-metal ferromagnets and low-T_c superconductors to this system should be taken carefully. This is because the high-spin polarization of the manganites, along with the *d*-wave pairing symmetry of the cuprate, points to a stronger weight of spin-dependent effects in transport compared to transition-metal structures.

In this paper, we examine a Co/YBCO/LCMO inverse superconducting spin switch. We exploit the natural oxidation of cobalt (Co) films to produce CoO/Co AF/F double layers that exhibit pronounced exchange bias, modifying the coercive field of the Co by several thousand oersteds. The CoO/Co layer also has a pronounced training effect, whereby the first magnetic hysteresis loop, after cooling from room temperature in a high magnetic field, has much higher coercive fields and sharper magnetization switching than, and so differs considerably from, the subsequent ones.[24–28] Measuring resistance vs. field sweeps at fixed temperatures along the superconducting transition, we find two distinct features. Positive MR peaks at the coercive fields of both the Co and the manganite can be ascribed to the effect of stray fields in all samples, whereas in samples with freshly deposited Co, we observe a well-defined MR *plateau* extending between the coercive fields of the LCMO and Co, determined by the AP alignment and probably related to spin-dependent transport.

After Co deposition, the YBCO cuprate at the interface shows a progressive deterioration (most likely a deoxygenation) until superconductivity completely disappears after a few weeks of exposure to the ambient. Nevertheless, in an intermediate stage, after a few days of depositing the Co, we can still observe a superconducting transition and the characteristic MR peaks at the coercive fields of the Co and LCMO, but without the MR *plateau* between them. We argue that the process ruining superconductivity also breaks the electronic coupling between ferromagnetic and superconducting layers at their interface. Consequently, also the spin-dependent scattering process at the interface is impeded that would give rise to the MR *plateau*. We extract the conclusion that while stray fields certainly cause positive MR peaks in inverse superconducting spin switches, an additional spin-dependent mechanism is also present, causing an MR *plateau* in fresh samples.

The structure of the paper is the following. In Sec. II, we give details of sample preparation and measurement conditions. Then we present results on the growth of Co on YBCO and describe a deterioration of the superconducting YBCO in contact with the Co layer, manifested by structural and transport properties shown by combined x-ray diffraction, temperature-dependent resistivity, and magnetization measurements. Then we present MR data on LCMO/YBCO and YBCO/Co bilayers, which exhibit MR peaks at coercivity. Next we describe the LCMO/YBCO/Co trilayer that shows an MR *plateau* between coercivities, along with the corresponding magnetization hysteresis loops showing exchange bias and training effects. Then we study the MR of the same trilayer, recorded over time, showing a deterioration of the YBCO layer. We discuss the results, focusing on the possible mechanisms giving rise to the magnetoresistance, in terms of stray fields (MR peaks) and spin-dependent transport (MR *plateau*).

II. EXPERIMENTAL DETAILS

Samples of LCMO and YBCO thin films were grown on (100) cut, polished $SrTiO_3$ (STO) substrates using a high-pressure dc-sputtering apparatus combining pure oxygen atmosphere (3.4 mbar) and high growth temperature (900 °C). This produces a slow (0.9 nm/min) and highly thermalized growth yielding good epitaxial properties. Further details about the growth can be found elsewhere.[29–31] Magnetization was measured using a vibrating sample magnetometer (VSM) using 2 mm vibration amplitude at 40 Hz.

Temperature-dependent (magneto)resistance was measured in the current in plane (CIP) geometry, with four contact pads in the four corners of the 5×5 mm^2 square samples, in a cryostat equipped with a 90 kOe magnet. The samples presented here have 15-nm-thick (40 u.c.) ferromagnetic LCMO electrodes. The plane of the film was aligned, utilizing the sensitive field dependence of the resistivity in the superconducting state, parallel to the applied 10 kOe magnetic field to approximately 0.05° with the help of a rotator. The resistivity measurements used a small (100 μA) dc current with reversing polarity to eliminate the effect of thermal voltages. The magnetic field, perpendicular to the current, was swept between ±10 kOe at fixed temperatures along the resistive transition, above and below the superconducting onset temperature. When MR is expressed in terms of percent, it is calculated as $MR\%=[(R_{max}-R_{min})/R_{min}]\times100$, where R_{max} is the maximum resistance value, taken typically at the coercivity peak, while R_{min} is the minimum value, between the MR peak and the high-field vortex background, reached typically at a few thousand Oe.

For heterostructures containing Co, 12-nm-thick Co films were deposited in a different vacuum chamber using dc magnetron sputtering in argon. Typically, no more than 4 h elapsed, with the sample in air, between terminating the oxide thin film deposition and commencing the metal deposition. After Co deposition, the chamber was backfilled with one atmosphere of O_2 to ensure a uniform growth of naturally oxidized CoO thin film on top of the Co. Immediately after Co deposition, the samples were transferred to the magnetoresistance setup, typically with delays not exceeding 2 h between terminating the Co deposition and cooling the sample below 100 K. After the magnetoresistance measurements, the magnetization was measured, again with as little delay as possible (2 h, typically).

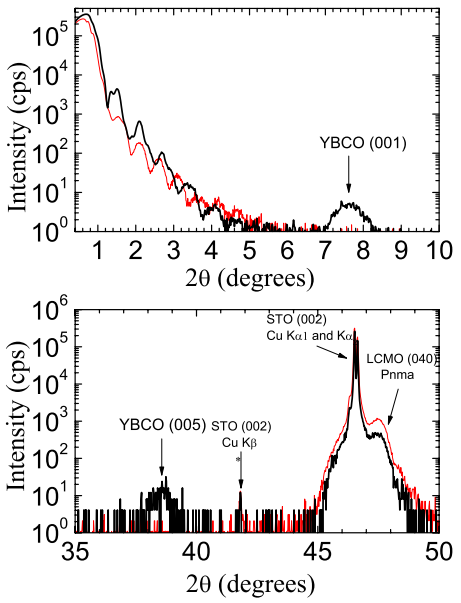

FIG. 1. (Color online) STO/LCMO/YBCO/Co sample in the fresh stage (thick, black line) and reacted stage (thin, red line). (Top) Low-angle reflectivity, the YBCO (001) diffraction is indicated, present only in the fresh stage. (Bottom) Bragg diffraction peaks, the YBCO (005) peak is indicated, present only in the fresh stage.

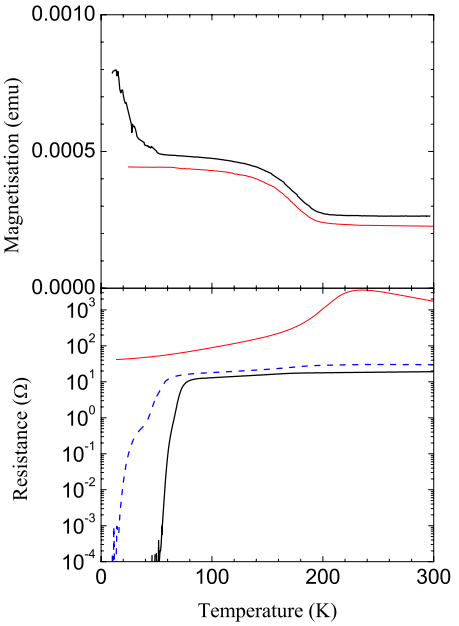

FIG. 2. (Color online) (Top) Magnetization vs temperature of the STO/LCMO/YBCO/Co trilayer sample in the fresh (thick, black line) and reacted stages (thin, red line). (Bottom) Resistance vs temperature without applied field in the fresh stage (thick, black line), intermediate stage (thick, dashed, blue line), and reacted stage (thin, red line).

Finally, samples were characterized by x-ray reflectometry and diffraction. To this purpose, θ-2θ scans were performed on a four-circle Bruker D8 diffractometer using Cu K_α radiation. Throughout the paper, fresh stage refers to the Co-containing samples and corresponding measurements taken after Co deposition (within 2 days), intermediate stage refers to measurements taken after approximately 2 weeks, whereas reacted stage refers to measurements taken after at least 2 months have elapsed.

III. RESULTS

The main focus of this study is the magnetoresistance of the LCMO/YBCO/Co trilayer. We first present structural and magnetic characterizations of the trilayer, highlighting the notable changes over time. Then we show the magnetoresistance of various bilayers, as they can be considered the constituent parts of a trilayer, although with the caveat that in a trilayer, the two F electrodes might be coupled magnetostatically.[16] Finally, we return to the trilayer and present its magnetoresistance and magnetization both immediately after deposition and after 2 weeks of aging.

A. Growth of Co on YBCO

We studied a STO/LCMO/YBCO/Co trilayer structure (where the STO indicates the substrate). X-ray diffraction and low-angle reflectivity provide structural information of the films, presented in Fig. 1. The top panel shows the low-angle x-ray reflectivity signal with the characteristic low-angle oscillations of thin films. At $2\theta \sim 7.5°$, the YBCO (001) reflection is clearly seen in the fresh stage (thick, black), but is absent in the reacted stage (thin, red). In the bottom panel, between 45° and 49° in 2θ, the substrate STO (002) and the LCMO *Pnma* (040) reflections are well identified and do not show appreciable change over time. At $2\theta \sim 37°$, for the fresh stage, the YBCO (005) peak is well identified, but in the reacted stage it is missing. Co deposited directly on YBCO apparently reacts slowly at the interface. Our structural data indicate that the YBCO structure is completely destroyed by *in situ* reaction with the Co. Probably, the Co extracts oxygen from the YBCO to form CoO on the YBCO side as well, similar to the other side of the Co film open to air.

Magnetization provides a measure of the changes of the amount of metallic Co over time. Magnetization vs. temperature of the STO/YBCO/Co sample is presented in the top panel of Fig. 2. The fresh stage (thick black curve) exhibits an upturn of the magnetization below $T_c \sim 50$ K, characteristic of these ferromagnetic-superconducting thin film samples in the superconducting state, referred to as paramagnetic Meissner-effect.[32] This upturn of the magnetization was measured with a VSM magnetometer. At this stage, we do not know if these upturns are artifacts due to a misalignment of the samples, but we believe they are connected to the presence of the ferromagnet. We never observe these upturns in samples not containing ferromagnetic layers. The Curie temperature of the LCMO film is ~200 K. Above 200 K, the high magnetization is due to the Co layer; as Co has a much higher Curie temperature, its contribution to the $M(T)$ of the sample is largely constant in the temperature window of the figure.

In the reacted stage (thin red curve), the contribution from the LCMO is unchanged. However, the low-temperature up-

turn, related to superconducting YBCO, is missing and the magnetization of the Co is reduced by *approximately* 15%. This indicates that approximately 15% of the Co turned into CoO during the 2 months between the two measurements, with the necessary oxygen taken both from the air and the YBCO.

Temperature-dependent resistance (Fig. 2, bottom panel) provides an indication of the quality of the YBCO sample via the overall resistance value and the superconducting transition temperature, T_{onset}. The latter indicates a progressive deterioration of the YBCO, it becomes lower with time, and is finally completely suppressed. Simultaneously, the normal-state resistance also increases with time.

In the fresh stage (thick, black curve), the zero field $R(T)$ shows a high $T_{onset} \sim 76$ K and low normal-state resistance that increases linearly with temperature, typical of high-quality YBCO thin films. The onset temperature is reduced due to proximity to two F layers.[30]

In the intermediate stage (thick, blue, dashed curve), T_{onset} is suppressed to 55 K, the transition is broadened, completed only at 10 K, with a large step in midtransition. This step in the resistance curves is indicative of a degraded layer close to the interface with reduced oxygen content. The normal-state resistance is also increased, compared to the fresh stage, but still varies linearly with temperature.

Finally, in the reacted stage (thin, red curve) the $R(T)$ shows only the characteristic metal-insulator transition behavior of LCMO, with a peak at $T_{\mathrm{Curie}} \sim 220$ K. The normal-state resistance also increases drastically, as both the effective Co and YBCO conductance channel widths decrease or disappear.

B. Bilayers

Bilayers did not exhibit the large positive MR peaks shown by trilayers with the same YBCO thickness, with either layer sequence STO/YBCO/LCMO, such that the YBCO was grown below the LCMO, with layer sequence STO/LCMO/YBCO, such that the YBCO was grown on top of the LCMO, or with layer sequence STO/YBCO/Co. In Fig. 3, we present the magnetoresistance of three different manganite-cuprate bilayers (panels on the left), exhibiting representative magnetoresistance behavior. The panels on the right show the corresponding temperature-dependent zero-field resistance curves for each sample, illustrating that for YBCO thickness greater than approximately 10 nm, the critical temperature is not suppressed by the presence of the ferromagnetic layer.

The panels on the top present transport data of a bilayer with the LCMO beneath the YBCO (STO/LCMO[15 nm]/YBCO[12 nm]). This is the bilayer structure (not the same bilayer though) that forms the basis of the trilayer structure studied in the preceding and next sections. The $R(H)$ was recorded at $T=56$ K, a temperature where the resistance is reduced compared to the normal-state value just above the T_{onset} as $R_{min}/R_n \sim 10^{-4}$. The zero-field resistance shows that $T_{onset} \sim 89$ K is close to the bulk value. At the coercive field ($H_c^F \sim 60$ Oe), a small MR peak of approximately 10%–20% is seen. Both the height of the MR peak and the coercive field are temperature dependent, though. The coercive field of manganite thin films increases at low temperature slowly, whereas the MR peak increases from 0 at T_{onset} to the 20% seen at the lowest temperature with measurable nonzero resistance.

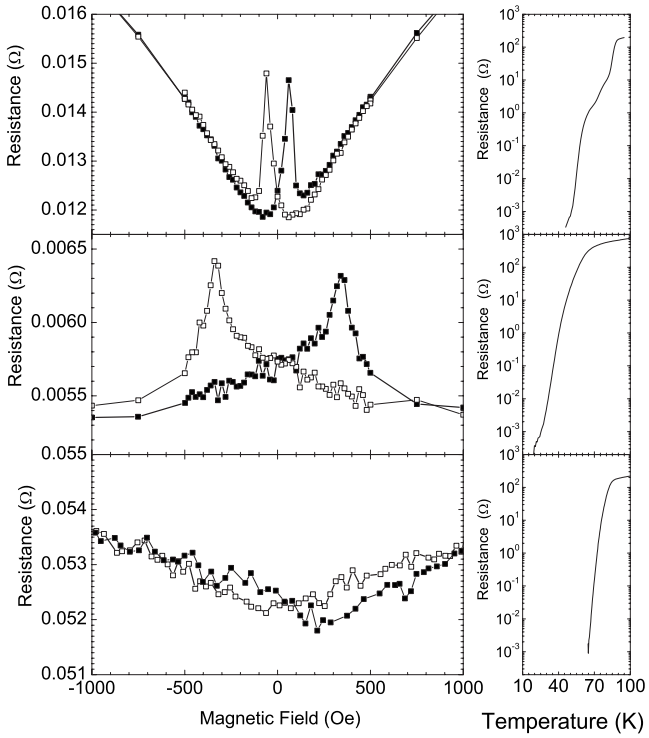

FIG. 3. Temperature-dependent resistance around the superconducting onset transition in $H=0$ (panels on the right) and MR below the onset, with $R_{min}/R_n \sim 10^{-4}$; the magnetic field is swept up (full symbols) and down (open symbols) (panels on left). (Top) Bilayer ($T=56$ K): STO/LCMO[15 nm]/YBCO[12 nm] with positive MR peaks at $H_c^F \sim \pm 60$ Oe. (Middle) Bilayer ($T=30$ K): STO/YBCO[5 nm]/LCMO[15 nm] with positive MR peaks at $H_c^F \sim \pm 340$ Oe. (Bottom) Bilayer ($T=69$ K): STO/YBCO[12 nm]/LCMO[15 nm] with no MR peaks at $H_c^F \sim \pm 200$ Oe.

It is worth emphasizing that these MR values are much smaller than the values found in STO/LCMO/YBCO/LCMO trilayers with similar thickness of the individual layers, for which MR may take values in excess of 1000%. This small MR is probably due to the effect of stray fields generated at the domain state of the ferromagnet. Domain structure in this sample geometry may be different than in bilayers with the YBCO underneath the LCMO and this is probably related to a small interface disorder. The smooth increase of the resistance at high magnetic field results from vortex dissipation. These vortices are perpendicular to the layers and are due to a small misalignment of the applied field out of the plane of the film.

The middle panels show data of a bilayer with the LCMO on top of the YBCO (STO/YBCO[5 nm]/LCMO[15 nm]) at $T=30$ K, below $T_{onset} \sim 67$ K, with $R_{min}/R_n \sim 10^{-5}$. It exhibits a small MR peak, at most 20%, at $H_c^F \sim 340$ Oe. The bottom panels show data of a bilayer with the LCMO on top of thicker YBCO (STO/YBCO[12 nm]/LCMO[15 nm]) at

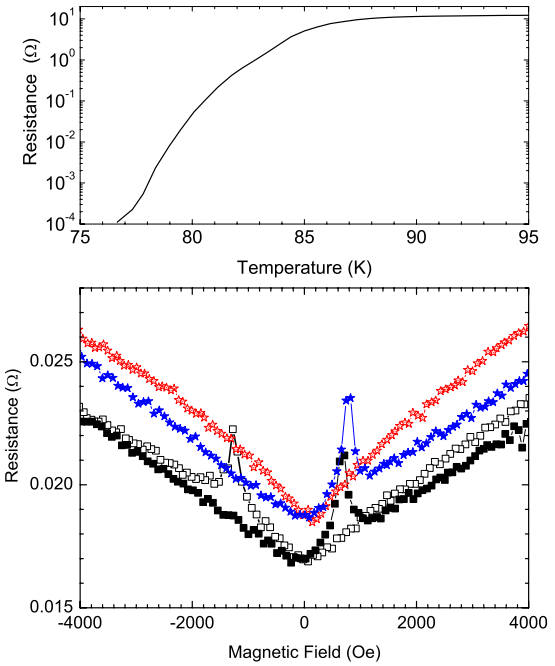

FIG. 4. (Color online) Co-coated YBCO film, STO/YBCO[12 nm]/Co[12 nm]. (Top) Temperature-dependent resistance around the superconducting onset transition in $H=0$ and (bottom) magnetoresistance below $T_{onset}=79$ K with $R_{min}/R_n \sim 10^{-3}$, cooled in $H=+40$ kOe. The magnetic field was first swept down from +40 to −10 kOe (red, open stars) then up to +10 kOe (blue, full stars). After several training cycles between ±10 kOe, the field was swept up (black, full squares) and down (black, open squares).

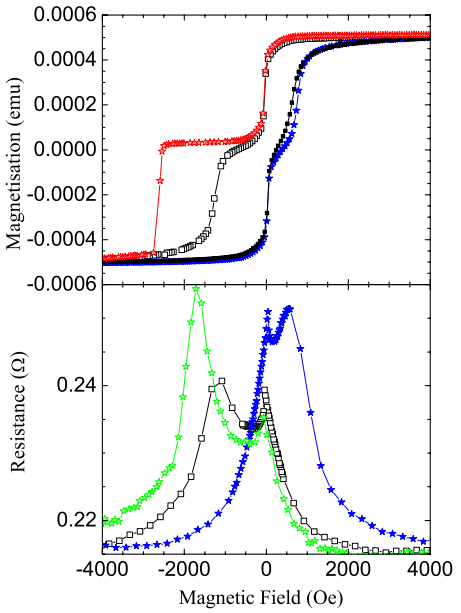

FIG. 5. (Color online) (Top) Magnetization hysteresis loops of the trilayer (STO/LCMO[15 nm]/YBCO [12 nm]/Co[12 nm]) in the fresh stage at $T=55$ K. Red, open stars show the first sweep down to −10 kOe after cooling in +10 kOe (untrained); blue, full stars show the subsequent up-sweep. Black squares show a hysteresis loop at the same temperature after many cycles (trained). (Bottom) Magnetoresistance of the same trilayer at $T=52$ K, $R_{min}/R_n \sim 10^{-2}$. Green open stars show the very first sweep, with magnetic field decreasing from +50 kOe. Blue full, stars show the subsequent sweep of the magnetic field up from −10 to +10 kOe. Black squares show the second sweep down of the magnetic field.

$T=69$ K, below $T_{onset} \sim 86$ K, with $R_{min}/R_n \sim 10^{-4}$. The salient feature of this data is the lack of positive MR peaks at the coercive field of the LCMO at $H_c^F \sim 200$ Oe. The absence of positive MR peaks points to a limited effect of stray fields for this layer sequence. This is most likely related to the atomically flat interfaces shown by electron microscopy observations and low-angle x-ray refinement in previous reports.[33,34]

We next present the magnetoresistance of a YBCO/Co bilayer (STO/YBCO[12 nm]/Co[12 nm]), at $T=79$ K, with $R_{min}/R_n \sim 10^{-3}$, cooled in $H=+40$ kOe, in Fig. 4. The Co thin film has rather high coercive field, increasing with lower temperature. The magnetoresistance exhibits sharp positive peaks, up to 50% at the lowest temperatures, at the coercive field of the Co. As the Co film is exposed to air, it develops an intentional antiferromagnetic CoO oxide layer. This layer has been shown to be 2–3 nm thick from x-ray reflectivity experiments.[24]

We studied the typical temperature-dependent coercive field, exchange bias, and training effect on samples of Co deposited on STO (not shown). CoO is an antiferromagnet and the Co/CoO bilayer is exchange biased.[24] The Co/CoO bilayer also exhibits a pronounced training effect, whereby after cooling from room temperature, the first magnetic field sweep has a very high coercive field, with sharp magnetization switching.[27,35] For the YBCO/Co sample, this untrained field sweep down from +40 to −10 kOe gives a barely visible positive MR peak at $H_c^F \sim 2300$ Oe (red, open stars). This is probably related to a domain nucleation process with all in-plane magnetization components (see below). The subsequent field sweep from −10 to +10 kOe has a pronounced positive MR peak at $H_c^F \sim 780$ Oe (blue stars). After several training cycles between ±10 kOe, the field was swept up (black, full squares) and down (black, open squares) with positive MR peaks at reduced coercive fields: $H_c^F \sim -1300$ Oe and $H_c^F \sim 690$ Oe.

The top panel of Fig. 4 shows the temperature-dependent resistance of the YBCO/Co bilayer, in zero external magnetic field. This measurement was performed within 1 day of depositing the Co. $T_{onset} \sim 86$ K of the YBCO is practically not affected by the subsequent ferromagnetic Co layer.

C. Trilayers

The main focus of this paper is the magnetoresistance of a LCMO/YBCO/Co trilayer immediately after Co deposition: in the fresh stage. We also present magnetization and magnetoresistance of the same sample after 2 weeks in air: in the intermediate stage. The temperature dependences of the superconducting transition in both fresh and intermediate stages are shown in Fig. 2.

The top panel of Fig. 5 shows the magnetization hysteresis loops of the trilayer (STO/LCMO[15 nm]/YBCO[12 nm]/Co[12 nm]) at $T=55$ K in the fresh stage. The red, open stars represent, after cooling in $H=+10$ kOe, the first sweep

of the magnetic field to $H=-10$ kOe (untrained), while the subsequent sweep back up to $H=+10$ kOe is shown by the blue, full stars. The black squares show a hysteresis loop at the same temperature after many cycles (trained). The sharp switching of the Co in the untrained loop at a high coercive field, $H_c^F \sim -2600$ Oe is notable. Similarly on the next upsweep, the switching is still sharp at a somewhat elevated coercive field $H_c^F \sim +750$ Oe compared to the fully trained hysteresis loop with coercive fields of approximately -1200 and $+600$ Oe and more rounded switching of the Co magnetization. The magnetization of the LCMO layer switches at $H_c^F \sim \pm 45$ Oe, independent of the training of the Co.

This asymmetry of the Co switching has been reported to result from different magnetization reversal mechanisms in the first and subsequent switches.[25] The first abrupt reversal is controlled by domain nucleation, while the more rounded subsequent reversals are due to magnetization rotation.[27,28,35] Magnetic force microscopy (MFM) observations show the micrometer-size domain structure appearing after the first magnetization reversal. Once formed, the ferromagnetic domains survive even at very large fields and cannot be erased by the application of a magnetic field in the direction of the cooling field. This provides experimental evidence supporting a change of the Co magnetization reversal after the first field switch.[35]

The origin of the large exchange bias is the coupling of the ferromagnetic domains to a large number of uncompensated moments at the boundaries between ten nanometer-size antiferromagnetic domains, given their difference in size.[36] When the magnetization of the ferromagnet is reversed, some of the interfacial uncompensated moments will change their orientation depending on their size and orientation with respect to the AF easy axis, i.e., not all magnetization vectors rotate back to their initial position so that the average AF interfacial magnetization is directed away from the cooling field at an angle that may be as large as 21°. This creates a torque on ferromagnetic spins and triggers the magnetization rotation mechanism.

For the thickness of the LCMO (15 nm) and Co (12 nm) chosen and their saturation magnetizations (3.6 and 3.8 μ_B per magnetic atom, respectively), their total magnetic moments are rather similar as indicated by the level of the *plateau* near $M=0$. The magnetic moments of the two ferromagnets are aligned antiparallel in the field range between the coercive fields of the LCMO and Co, that is, in the region of the *plateau*. In this field range, neither the LCMO nor the Co magnetization changes; there are no domain-wall movements. The very first hysteresis loop after cooling in a large field provides a very broad *plateau*. This offers us an experimental situation where any effects related to the magnetization switching at the coercive field can be decoupled from effects due to AP alignment of the magnetization.

The bottom panel of Fig. 5 displays the magnetoresistance of the trilayer at $T=52$ K and a resistance drop of $R_{min}/R_n \sim 10^{-2}$ in the fresh stage. The green, open stars show the very first sweep, with magnetic field decreasing from $+50$ kOe (the field in which the sample was cooled down to 52 K). There are two large positive MR peaks corresponding to the switching of the LCMO and Co at approximately -40 and -1750 Oe, respectively. The blue, full stars represent the subsequent sweep of the magnetic field up, with the MR peaks at approximately $+40$ and $+550$ Oe. Finally, the black squares show the second sweep down of the magnetic field. The Co is now trained, with the MR peaks at approximately -40 Oe for LCMO and at a reduced coercive field of approximately -1100 Oe for the Co. The LCMO has a coercive field of approximately ± 40 Oe, independent of the training and exchange bias of the Co.

The coercive fields of the Co (LCMO) are marked by broad (sharp) peaks in the magnetoresistance. Crucially, between the two coercive fields of the respective ferromagnetic layers, the resistance remains considerably higher than the background level, even in the case of the black curve, where the Co and the LCMO MR peaks are farthest separated. This is the sought after AP *plateau*. The size of the MR *plateau* presented in Fig. 5 is only approximately 30% because the data were taken closer to the resistive onset, at $R_{min}/R_n \sim 10^{-2}$. The MR becomes larger than 100% when the temperature is reduced such that $R_{min}/R_n \sim 10^{-4}$. It increases exponentially with decreasing R_{min}/R_n below the resistive onset, similar to LCMO/YBCO/LCMO trilayers[37] (not shown).

The untrained hysteresis loop of the R vs. H experiment has a reduced coercive field compared to the magnetic hysteresis loop at comparable temperature. There is a technical reason for this apparent discrepancy. In this experiment, the sample had to be realigned at 52 K after cooling from 300 K to make it exactly parallel to the field, as the rotator may move approximately half a degree on temperature cycling. The realignment involves rotating the sample in the $H=50$ kOe field by as much as 10°, a process that is detrimental to the above-described mechanism of F-AF domain coupling. Therefore, one ought not to conclude that the MR peak would appear in the region of AP alignment.

Next, we contrast the magnetoresistance of the fresh and intermediate stages of the LCMO/YBCO/Co trilayer. We observed drastic changes, related to the deterioration of the YBCO, detailed in Sec. I. As Fig. 6 shows, the magnetoresistance displays sharp peaks at the coercive fields of the ferromagnetic layers. However, the elevated resistance between them, the AP *plateau*, seen in the fresh stage of Fig. 5, is completely absent. As Fig. 2 demonstrates, in the intermediate stage, the superconducting onset is drastically reduced and even displays a step around 35 K. The bottom panel of Fig. 6 shows the magnetoresistance of the intermediate stage trilayer sample at 25 K with $R_{min}/R_n \sim 10^{-3}$. At the coercive fields of Co and LCMO, the magnetoresistance has peaks of approximately 10% that are sharper than in the fresh stage.

The red, open stars represent the untrained sweep, recorded after cooling with $+50$ kOe parallel to the film; here the Co peak is at $H_c^F \sim -4000$ Oe. The coercive field of the untrained sweep is much larger than in the other figures due to the reduced temperature. In fact, we observed that at 10 K, this coercive field can increase up to the surprisingly large value of -8000 Oe. Data of the blue, full stars were recorded afterwards, with the Co peak at $H_c^F \sim 900$ Oe, whereas data of the black, open squares were recorded after training the Co, with the Co peak at $H_c^F \sim -2200$ Oe.

Note that the height of the MR peaks at the Co coercive field is considerably weaker in the first field down sweep

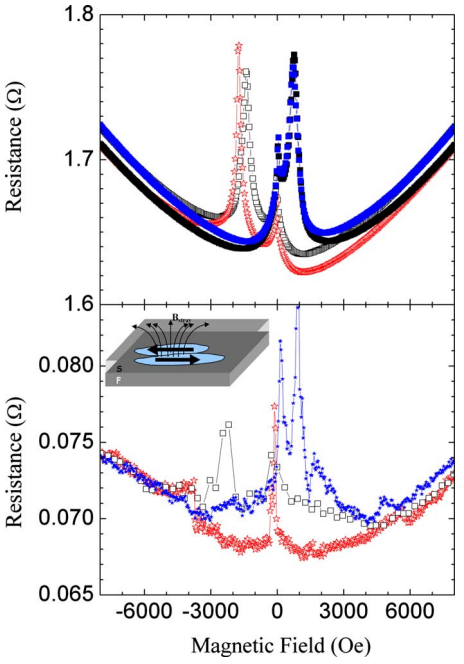

FIG. 6. (Color online) Magnetoresistance of the trilayer sample in the intermediate stage at 47 K with $R_{min}/R_n \sim 10^{-1}$ (top) and at 25 K with $R_{min}/R_n \sim 10^{-3}$ (bottom). Red, open stars show the first sweep down to −10 kOe after cooling in +50 kOe (untrained); blue, full stars show the subsequent up-sweep. Black squares show a hysteresis loop at the same temperature after many cycles (trained). The cartoon shows how the stray fields emerging at the domain walls may penetrate perpendicularly the superconducting film.

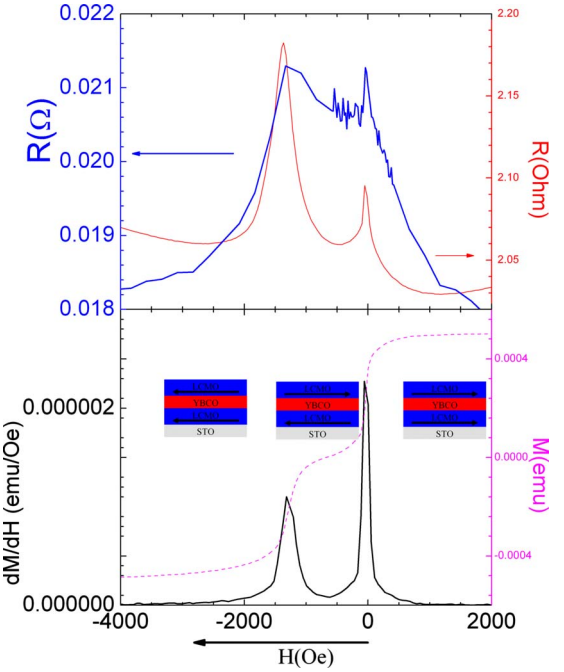

FIG. 7. (Color online) (Top) Magnetoresistance of the trilayer in the fresh (thick blue line) and intermediate (thin red line) stages. (Bottom) Magnetization vs field (thin dashed purple line) and its derivative (thick solid black line) in the fresh stage. All data were recorded at 48 K on sweeping down the magnetic field. The cartoons show the orientation of the magnetizations of the two LCMO layers at the various field regions.

than in subsequent sweeps. On the contrary, the LCMO peak, at approximately ±130 Oe at this low temperature, is not modified substantially from up to down field sweeps, independent of the Co training. This can be explained in view of the change of the Co magnetization reversal mechanism after the first field switch from domain nucleation to magnetization rotation in large domains. It is reasonable that magnetization rotation may in fact change the intensity of the stray fields and thus the height of MR peaks (see inset of Fig. 6). Importantly, between the coercive fields of Co and LCMO, there is no MR *plateau*, certainly in the case of sweeping the field down, when the peaks are well separated.

The top panel of Fig. 6 shows the magnetoresistance of the same trilayer in the intermediate stage above the step of the resistive transition at 47 K (see Fig. 2), with $R_{min}/R_n \sim 10^{-1}$. The color coding of the sweeps is the same as in the bottom panel, showing the Co peak at different coercivities, reflecting the progressive training and exchange bias of the CoO/Co. The LCMO coercive fields are approximately ±50 Oe. The Co coercive fields are approximately −1700, −1400, and +700 Oe for the untrained and trained down- and up-sweeps, respectively. Importantly, there is no hint of a *plateau* between the LCMO and Co coercive fields. As the MR peaks are approximately 10% high at both 47 and 25 K, they do not display the exponential growth with decreasing R_{min}/R_n, contrary to the behavior seen in the fresh stage or in LCMO/YBCO/LCMO trilayers in Refs. 9 and 37.

Finally, in Fig. 7, the MR in the fresh (thick blue line) and intermediate (thin red line) stages in the top panel are contrasted to each other and to the derivative (thick black line) of the magnetization hysteresis curve (thin dashed purple line) in the bottom panel. Only the down sweeps with decreasing field are shown for simplicity. All data were recorded at 48 K in order to obtain the same coercive field of the trained Co layer, although this way the overall resistance in the intermediate stage remains quite high. In the fresh stage, there is a well-defined *plateau* between, and relatively small peaks at, the coercive fields of the LCMO and Co. In contrast, in the intermediate stage, there are well-defined peaks at each coercive field. Furthermore, the peak width of the intermediate stage corresponds well to the width of the derivative of the magnetization hysteresis curve at both the LCMO and Co coercive fields.

IV. DISCUSSION

We have shown that magnetization switching is accompanied by MR peaks pointing to an effect of stray fields on the superconductivity of the YBCO layer. It is clear, also, that specific domain configurations create magnetic fields affecting superconductivity differently as shown by the different behavior exhibited by magnetoresistance with untrained vs. trained Co in the intermediate stage. However, samples in the fresh stage have an additional, well-defined MR *plateau* between the two coercive fields, which we attribute to a spin-dependent effect related to the antiparallel orientation of the ferromagnetic layers.

We have previously proposed that spin-dependent quasiparticle scattering at the F/*S* interface of LCMO/YBCO/LCMO samples that is enhanced in the AP configuration may modulate the superconductivity giving rise to the large MR peaks.[9,37] The smaller MR values at the *plateau* (30%–100%) in LCMO/YBCO/Co as compared to the large values found in symmetric LCMO/YBCO/LCMO trilayers in excess of 300% at similar R_{min}/R_n may be related to the smaller degree of spin polarization of the conduction band of the Co (34%) contrary to the high spin polarization of LCMO.[38,39]

The effect of stray fields on the superconducting state has been extensively discussed by Steiner and Ziemann and by Stamopoulos *et al.*[12,16] Steiner and Ziemann studied F/*S* bilayers (Nb/Fe), F/*S*/F trilayers (Co/Nb/Fe), and EB-F/*S*/F exchange biased trilayers (CoO/Co/Nb/Fe). They found positive MR peaks (or equivalently depressions of T_c) at the coercive field(s) of the ferromagnet(s) in bilayers and trilayers and proposed that they originate in the micromagnetic stray fields of the ferromagnetic layers.

Stray fields generated at coercivity emerge all over the surface of the ferromagnet (and should not be confused by stray fields appearing at the edges of a homogenously magnetized ferromagnet). It has been proposed that these stray fields mediate a magnetic (magnetostatic) coupling mechanism in which transverse field lines pierce the superconductor giving rise to resistive dissipation.[13] According to Stamopoulos *et al.*[16] this mechanism should be maximal when the coercive fields of the two ferromagnets are very similar, coupling domains that emerge simultaneously in both ferromagnets. In contrast, when the coercive fields are different, the stray-field-mediated coupling is less pronounced. This, again according to Stamopoulos *et al.*,[16] would explain the smaller MR values observed in NiFe/Nb/NiFe samples with one of the layers pinned by exchange bias. Exchange bias maintains an in-plane magnetization, thus it restricts the out of plane magnetization rotation (necessary for the occurrence of broad dissipation peaks) to a small magnetic field range around coercivity.

Therefore, in view of the large exchange bias and very different values of the coercivities found in LCMO/YBCO/Co samples, it is hard to conceive of a magnetostatic coupling between domain states of top and bottom ferromagnets that might be effective. Stamopoulos *et al.*[16] predicted strong magnetostatic coupling and intensive MR peaks in F/*S*/F trilayers when the coercive fields of the two F electrodes are comparable. It is clear, however, that magnetization rotation in the trained state is an important ingredient for the occurrence of MR peaks at coercivity also in our samples. In this regard, it is worthwhile to recall that in the intermediate stage the MR in the very first (untrained) field sweep showed essentially no or very small MR peaks.

The first domain state in untrained Co films is known to occur by domain nucleation with magnetization components only parallel and antiparallel to field. This conclusion has been reported to follow from very small or absent anomalous MR (AMR) peaks at coercivity found in single-layer CoO/Co samples for current injected perpendicular to field.[24,26,27] Since AMR scales with $1-\cos^2(\theta)$, with θ being the angle between current and magnetization, domain nucleation with magnetizations exactly parallel or antiparallel to field would yield $\cos^2(\theta)=1$ and thus no measurable change in AMR at coercivity. Subsequent sweeps yield comparable AMR peaks, in CoO/Co, at both coercive fields reflecting that reversal now occurs by magnetization rotation, as also indicated by the more rounded hysteresis loops.

The MR peaks associated with Co are considerably sharper in the intermediate stage than in the fresh stage and this is especially pronounced in the more trained sweep. This is a remarkable result if one takes into account that training is accompanied by larger participation of rotation in magnetization switching, which would widen the MR peaks. Since an oxide barrier layer forms between Co and YBCO with aging, closure of field lines within the oxide layer might be the cause of the sharper MR peaks because the weak magnetic flux from the incipient domain state is effectively damped by the oxide. The diamagnetic screening by the superconductor of the component of the stray field perpendicular to the layers can also be ruled out since this effect is expected to be larger in the fresh sample. The change in MR peak width may thus be a reflection of an additional mechanism in the fresh stage originating at the alignment state of the magnetization of the F electrodes. As the magnetization reversal process is very different in LCMO from that in Co, similar differences between first and subsequent LCMO switchings are not seen in the related MR.

The *plateau* exhibited in the fresh stage (see Figs. 5 and 7) of the LCMO/YBCO/Co trilayer is then characterized as having an intrinsic spin-dependent transport origin. For this mechanism, rather transparent and smooth interfaces are required between the ferromagnets and the superconductor. This point is shown up by the observation of the lack of a *plateau* in the intermediate stage (see Figs. 6 and 7), where an oxide barrier is assumed to form between superconducting YBCO and ferromagnetic Co. As the chemical reaction between Co and YBCO slowly progresses, the interface necessarily deteriorates and so only the small, positive MR peaks at coercivity remain, again characterized according to Steiner and Ziemann as having an extrinsic origin, such as stray fields.[12]

Interface roughness is an additional source of stray fields and thus of MR peaks. In flat layers with in-plane magnetization, the field induced in the superconductor would be very small and only due to finite-size effects which may be enhanced in the domain state. This is the reason why in very smooth bilayers, with LCMO on top, switching effects are absent. Small MR peaks appear, however, in bilayers with LCMO on the bottom. van Zalk *et al.* showed recently, by using finite element simulations, that at rough F/*S* interfaces, substantial magnetic field penetrates into the superconductor.[40]

The field induced due to the rough surface of the ferromagnet ("orange peel" effect) will be directed opposite to the magnetization and may thus be parallel or antiparallel to the applied field depending on the stage of the sweep, essentially causing a decreased effective field at saturation and an enhanced field after crossing zero field but still before switching. At large field, the resistance will be lower than in bare YBCO films due to roughness, as stray fields become AP to the applied field. A resistance increase occurs when external

and stray fields point in the same direction. Thus at coercivity, there is a down shift of the resistance curve due to a partial cancellation of the external field by the antiparallel stray fields making magnetoresistance change at coercivity to resemble more a step than a peak. Note, however, that in our case, MR peaks at coercivity are quite sharp pointing to magnetization rotation at coercivity as the dominant source of the stray fields.

V. CONCLUSIONS

In summary, we have examined the inverse superconducting spin switch behavior of Co/YBCO/LCMO structure. We have used the naturally forming CoO/Co AF/F double layers to magnetically pin the Co layer by exchange bias allowing the modification of the coercive field of the Co by several thousand oersteds. Measuring resistance vs. field sweeps at fixed temperatures along the superconducting transition, we found positive MR peaks occurring at the coercive fields of both the Co and the LCMO which can be unambiguously ascribed to the effect of stray fields generated at the domain state of the ferromagnet. The pronounced training effect of the CoO/Co layer, originating in a larger participation of magnetization rotation within domains in magnetization switching, also has a strong effect on MR peaks, showing that specific domain configurations create stray fields affecting superconductivity differently. In samples with freshly deposited Co, we observe an additional, well-defined MR *plateau* extending between the coercive fields of the LCMO and Co, determined by the AP alignment. This *plateau* disappears with time due to the formation of a nonsuperconducting oxide layer at the YBCO/Co interface that breaks the electronic coupling between the ferromagnet and the superconductor. We extract the conclusion that while stray fields certainly cause positive MR peaks in inverse superconducting spin switches, an additional mechanism is also present possibly related to the spin-dependent quasiparticle scattering at the F/*S* interface proposed for LCMO/YBCO/LCMO samples that is enhanced in the AP configuration.

ACKNOWLEDGMENTS

We thank A. Goldman for fruitful discussions within the framework of the joint US-Spain NSF Materials World Network Grant No. 709584. This work has been carried out with the support of the "Ramon y Cajal" contract and Grant No. MAT2007-30922E and MAT2008–06517 of the Spanish Ministry for Science and Innovation.

*nmnemes@fis.ucm.es

[1] A. I. Buzdin, Rev. Mod. Phys. **77**, 935 (2005).
[2] F. S. Bergeret, A. F. Volkov, and K. B. Efetov, Rev. Mod. Phys. **77**, 1321 (2005).
[3] J. Y. Gu, C. Y. You, J. S. Jiang, J. Pearson, Y. B. Bazaliy, and S. D. Bader, Phys. Rev. Lett. **89**, 267001 (2002).
[4] A. Potenza and C. H. Marrows, Phys. Rev. B **71**, 180503(R) (2005).
[5] I. C. Moraru, W. P. Pratt, and N. O. Birge, Phys. Rev. Lett. **96**, 037004 (2006).
[6] F. Giazotto, F. Taddei, F. Beltram, and R. Fazio, Phys. Rev. Lett. **97**, 087001 (2006).
[7] G. X. Miao, K. S. Yoon, T. S. Santos, and J. S. Moodera, Phys. Rev. Lett. **98**, 267001 (2007).
[8] G.-X. Miao, A. V. Ramos, and J. S. Moodera, Phys. Rev. Lett. **101**, 137001 (2008).
[9] V. Pena, Z. Sefrioui, D. Arias, C. Leon, J. Santamaria, J. L. Martinez, S. G. E. te Velthuis, and A. Hoffmann, Phys. Rev. Lett. **94**, 057002 (2005).
[10] A. Y. Rusanov, S. Habraken, and J. Aarts, Phys. Rev. B **73**, 060505(R) (2006).
[11] A. Singh, C. Surgers, and H. v. Lohneysen, Phys. Rev. B **75**, 024513 (2007).
[12] R. Steiner and P. Ziemann, Phys. Rev. B **74**, 094504 (2006).
[13] D. Stamopoulos, E. Manios, and M. Pissas, Phys. Rev. B **75**, 014501 (2007).
[14] L. Y. Zhu, T. Y. Chen, and C. L. Chien, Phys. Rev. Lett. **101**, 017004 (2008).
[15] A. Y. Aladyshkin, A. V. Silhanek, W. Gillijns, and V. V. Moshchalkov, Supercond. Sci. Technol. **22**, 053001 (2009).
[16] D. Stamopoulos, E. Manios, and M. Pissas, Supercond. Sci. Technol. **20**, 1205 (2007).
[17] P. Przyslupski, A. Tsarou, P. Dluzewski, W. Paszkowicz, R. Minikayev, K. Dybko, M. Sawicki, B. Dabrowski, and C. Kimball, Supercond. Sci. Technol. **19**, S38 (2006).
[18] K. Senapati and R. C. Budhani, Phys. Rev. B **71**, 224507 (2005).
[19] J. Hoppler *et al.*, Nature Mater. **8**, 315 (2009).
[20] J. Chakhalian *et al.*, Nat. Phys. **2**, 244 (2006).
[21] S. Soltan, J. Albrecht, and H. U. Habermeier, Phys. Rev. B **70**, 144517 (2004).
[22] H. Habermeier, G. Cristiani, R. Kremer, O. Lebedev, and G. van Tendeloo, Physica C **364**, 298 (2001).
[23] C. Visani, Ph.D. thesis, Universidad Complutense de Madrid, 2010.
[24] F. Radu, M. Etzkorn, R. Siebrecht, T. Schmitte, K. Westerholt, and H. Zabel, Phys. Rev. B **67**, 134409 (2003).
[25] M. Gruyters and D. Riegel, Phys. Rev. B **63**, 052401 (2000).
[26] T. Gredig, I. Krivorotov, and E. Dahlberg, J. Appl. Phys. **91**, 7760 (2002).
[27] S. Brems, K. Temst, and C. Van Haesendonck, Phys. Rev. Lett. **99**, 067201 (2007).
[28] A. Hoffmann, Phys. Rev. Lett. **93**, 097203 (2004).
[29] Z. Sefrioui, M. Varela, V. Pena, D. Arias, C. Leon, J. Santamaria, J. E. Villegas, J. L. Martinez, W. Saldarriaga, and P. Prieto, Appl. Phys. Lett. **81**, 4568 (2002).
[30] Z. Sefrioui, D. Arias, V. Pena, J. E. Villegas, M. Varela, P. Prieto, C. Leon, J. L. Martinez, and J. Santamaria, Phys. Rev. B **67**, 214511 (2003).
[31] V. Pena, Z. Sefrioui, D. Arias, C. Leon, J. Santamaria, M. Varela, S. J. Pennycook, and J. L. Martinez, Phys. Rev. B **69**, 224502 (2004).
[32] M. A. Lopez de la Torre, V. Pena, Z. Sefrioui, D. Arias, C. Leon,

J. Santamaria, and J. L. Martinez, Phys. Rev. B **73**, 052503 (2006).
[33] J. Santamaria, M. E. Gomez, J. L. Vicent, K. M. Krishnan, and I. K. Schuller, Phys. Rev. Lett. **89**, 190601 (2002).
[34] M. Varela, A. Lupini, S. Pennycook, Z. Sefrioui, and J. Santamaria, Solid-State Electron. **47**, 2245 (2003).
[35] S. Brems, A. Volodin, C. Van Haesendonck, and K. Temst, J. Appl. Phys. **103**, 113912 (2008).
[36] J. Nogues and I. K. Schuller, J. Magn. Magn. Mater. **192**, 203 (1999).
[37] N. M. Nemes *et al.*, Phys. Rev. B **78**, 094515 (2008).
[38] M. H. Jo, N. D. Mathur, N. K. Todd, and M. G. Blamire, Phys. Rev. B **61**, R14905 (2000).
[39] Z. Sefrioui, V. Cros, A. Barthelemy, V. Pena, C. Leon, J. Santamaria, M. Varela, and S. J. Pennycook, Appl. Phys. Lett. **88**, 022512 (2006).
[40] M. van Zalk, M. Veldhorst, A. Brinkman, J. Aarts, and H. Hilgenkamp, Phys. Rev. B **79**, 134509 (2009).